

Structural and Natural Isotopic Abundance Analysis of Magnesium Gluconate Treated with Energy of Consciousness (The Trivedi Effect[®]) Using LC-MS and NMR

Mahendra Kumar Trivedi¹, Alice Branton¹, Dahryn Trivedi¹, Gopal Nayak¹, Aileen Carol Lee¹, Aksana Hancharuk¹, Carola Marina Sand¹, Debra Jane Schnitzer¹, Rudina Thanasi¹, Eileen Mary Meagher¹, Faith Ann Pyka¹, Gary Richard Gerber¹, Johanna Catharina Stromsnas¹, Judith Marian Shapiro¹, Laura Nelson Streicher¹, Lorraine Marie Hachfeld¹, Matthew Charles Hornung¹, Patricia M. Rowe¹, Sally Jean Henderson¹, Sheila Maureen Benson¹, Shirley Theresa Holmlund¹, Stephen P. Salters¹, Parthasarathi Panda², Kalyan Kumar Sethi², Snehasis Jana^{2,*}

¹Trivedi Global, Inc., Henderson, Nevada, USA

²Trivedi Science Research Laboratory Pvt. Ltd., Bhopal, Madhya Pradesh, India

Email address:

publication@trivedieffect.com (S. Jana)

*Corresponding author

To cite this article:

Mahendra Kumar Trivedi, Alice Branton, Dahryn Trivedi, Gopal Nayak, Aileen Carol Lee, Aksana Hancharuk, Carola Marina Sand, Debra Jane Schnitzer, Rudina Thanasi, Eileen Mary Meagher, Faith Ann Pyka, Gary Richard Gerber, Johanna Catharina Stromsnas, Judith Marian Shapiro, Laura Nelson Streicher, Lorraine Marie Hachfeld, Matthew Charles Hornung, Patricia M. Rowe, Sally Jean Henderson, Sheila Maureen Benson, Shirley Theresa Holmlund, Stephen P. Salters, Parthasarathi Panda, Kalyan Kumar Sethi, Snehasis Jana. Structural and Natural Isotopic Abundance Analysis of Magnesium Gluconate Treated with Energy of Consciousness (The Trivedi Effect[®]) Using LC-MS and NMR. *Chemical and Biomolecular Engineering*. Vol. 2, No. 3, 2017, pp. 124-134. doi: 10.11648/j.cbe.20170203.11

Received: January 31, 2017; **Accepted:** February 14, 2017; **Published:** March 9, 2017

Abstract: The current research article was aimed to investigate the impact of The Trivedi Effect[®] - Energy of Consciousness Healing Treatment on the structural properties and isotopic abundance ratio (P_{M+1}/P_M and P_{M+2}/P_M) of magnesium gluconate using LC-MS and NMR spectroscopy. Magnesium gluconate was divided into two parts – one part was control, and another part was treated with The Trivedi Effect[®] remotely by eighteen renowned Biofield Energy Healers and defined as the Trivedi Effect[®] Treated sample. The liquid chromatogram of the control sample showed two peaks at R_t of 1.81 and 2.06 min, whereas the Trivedi Effect[®] Treated sample displayed these peaks at R_t of 1.79 and 2.03 min. The ESI-MS spectra of the control and the Trivedi Effect[®] Treated samples revealed the presence of the mass for magnesium gluconate ion in two forms at m/z 447 (adduct form with methanol) and 415 (protonated ion) in positive ionization mode. But, it showed the mass for the gluconate ion at m/z 195 in the negative ionization mode. The fragmentation pattern of magnesium gluconate in the treated sample was notably altered as compared to the control sample. The proton and carbon signals for CH, CH₂ and CO groups in the proton and carbon NMR spectra were found almost similar for the control and the treated samples. The isotopic abundance ratio analysis revealed that the isotopic abundance ratio of P_{M+1}/P_M (²H/¹H or ¹³C/¹²C or ¹⁷O/¹⁶O or ²⁵Mg/²⁴Mg) in two magnesium gluconate ion forms at m/z 447 and 415 in treated sample was significantly decreased by 59.82% and 55.44%, respectively compared with the control sample. The percentage change in the isotopic abundance ratio of P_{M+2}/P_M (¹⁸O/¹⁶O or ²⁶Mg/²⁴Mg) was remarkably decreased in the magnesium gluconate ion at m/z 447 in the treated sample by 78.26% compared with the control sample. Consequently, the isotopic abundance ratio of P_{M+1}/P_M (²H/¹H or ¹³C/¹²C or ¹⁷O/¹⁶O) in gluconate ion in the treated sample was significantly increased by 37.35% with respect to the control sample. Thus, the Trivedi Effect[®] treated magnesium gluconate could be valuable for designing better pharmaceutical and/or nutraceutical formulations through its changed physicochemical and thermal properties, which might be providing better therapeutic response against various diseases such as diabetes mellitus, allergies, aging, inflammatory diseases, immunological disorders, and other chronic infections. The treated magnesium gluconate might be helpful to design the novel potent enzyme inhibitors by using its kinetic isotope effects.

Keywords: Consciousness Energy Healing Treatment, Biofield Energy Healers, The Trivedi Effect®, Magnesium Gluconate, LC-MS, NMR, Isotopic Abundance Ratio, Isotope Effects

1. Introduction

The Magnesium ion (Mg^{2+}) is a major intracellular divalent cation. It is an essential mineral for several enzymes, DNA and RNA synthesis, reproduction and protein synthesis as well as a vital coherent controller of glycolysis and the Krebs cycle [1, 2]. Magnesium gluconate ($C_{12}H_{22}MgO_{14}$) is the organometallic salt of magnesium with gluconic acid produced from glucose catalyzed by glucose oxidase [3]. Magnesium gluconate is found to be the most powerful antioxidant than other magnesium salts and it is useful for the prevention and treatment of many diseases such as cardiovascular diseases, diabetes, allergies, inflammatory diseases, immunological disorders, Alzheimer's disease, asthma, pre-eclampsia and eclampsia, cancer, etc. [4-8]. It can be used as neuroprotective [9], for the treatment of oxidative stress induced ischemia/reperfusion injury [10] and also labor in women arrested initially with intravenous therapy as an oral tocolytic agent [11]. Magnesium gluconate showed the highest bioavailability and most physiologically acceptable salt among other magnesium salts like chloride, sulfate, carbonate, acetate, citrate, lactate, aspartate, etc. [8, 12]. This treated magnesium gluconate mineral can be for the prevention and treatment of various human diseases.

Since ancient times, many different cultures, religions and systems of belief have recognized a living force that preserves and inhabits every living organism. This force is the source of 'life' and has been called various names, such as prana by the Hindus, *qi* or *chi* by the Chinese, and *ki* by the Japanese. This is believed to correlate with the soul, spirit and mind. This hypothetical vital force has been scientifically evaluated and is now considered the Bioenergetics Field. The Biofield Energy is a dynamic electromagnetic field surrounding the human body, resulting from the continuous emission of low-level light, heat, and acoustical energy from the body. Biofield Energy is infinite, paradimensional and can freely flow between the human and environment [13, 14]. So, a human has the ability to harness energy from the ionosphere of the earth, the "universal energy field", and transmit it to any living organism(s) or nonliving object(s) around the globe. The object or recipient always receives the energy and responds in a useful way. This process is known as The Trivedi Effect® - Biofield Energy Healing Treatment [15, 16]. Biofield (Putative Energy Field) based Energy Therapies are used worldwide to promote health and healing. The National Center of Complementary and Integrative Health (NCCIH) has recognized and accepted Biofield Energy Healing as a Complementary and Alternative Medicine (CAM) health care approach in addition to other therapies, medicines and practices such as natural products, deep breathing, yoga, Tai Chi, Qi Gong, chiropractic/osteopathic manipulation, meditation, massage,

special diets, homeopathy, progressive relaxation, guided imagery, acupressure, acupuncture, relaxation techniques, hypnotherapy, healing touch, movement therapy, pilates, rolfing structural integration, mindfulness, Ayurvedic medicine, traditional Chinese herbs and medicines, naturopathy, essential oils, aromatherapy, Reiki, cranial sacral therapy and applied prayer (as is common in all religions, like Christianity, Hinduism, Buddhism and Judaism) [17]. Biofield Energy Treatment (The Trivedi Effect®) has been extensively studied with significant outcomes in many scientific fields such as cancer research [18, 19], altered antimicrobial sensitivity of pathogenic microbes in microbiology [20, 21], genetics [22, 23], biotechnology [24, 25], altered physical and chemical properties of pharmaceuticals [26, 27], nutraceuticals [28, 29], improved overall growth and yield of plants in agricultural science [30, 31], and changing the structure of the atom in relation to various metals, ceramics, polymers and chemicals in materials science [32-35]. The scientific study indicated that Biofield Energy Healing Treatment (The Trivedi Effect®) might be an alternate method for increasing or decreasing the natural isotopic abundance ratio of the substances [36, 37]. The stable isotope ratio analysis has the wide applications in several scientific fields for understanding the isotope effects resulting from the variation of the isotopic composition of the molecule [38, 39]. Conventional mass spectrometry (MS) techniques such as liquid chromatography – mass spectrometry (LC-MS), gas chromatography – mass spectrometry (GC-MS) are widely used for isotope ratio analysis with sufficient precision [40]. Hence, LC-MS and NMR (Nuclear Magnetic Resonance) were used in this study to characterize the structural properties of the Biofield Energy Treated and untreated magnesium gluconate for the quality control purpose in pharmaceutical and nutraceutical industries. Consequently, LC-MS based isotopic abundance ratio (P_{M+1}/P_M and P_{M+2}/P_M) analysis in both The Trivedi Effect®- treated and untreated samples was aimed to investigate the influence of The Trivedi Effect® - Consciousness Energy Healing Treatment on the isotopic abundance ratio in magnesium gluconate.

2. Materials and Methods

2.1. Chemicals and Reagents

Magnesium gluconate hydrate was purchased from Tokyo Chemical Industry Co., Ltd. (TCI), Japan. All other chemicals used in the experiment were of analytical grade available in India.

2.2. Energy of Consciousness Healing Treatment Strategies

Magnesium gluconate was one of the components of the

new proprietary herbomineral formulation, which was developed by our research team and was used *per se* as the test compound for the current study. The test compound was divided into two parts, one part of the test compound was treated with the Energy of Consciousness by eighteen renowned Biofield Energy Healers (The Trivedi Effect[®]) and defined as Biofield Energy Treated or The Trivedi Effect[®] treated sample, while the second part of the test compound did not receive any sort of treatment and was defined as the untreated or control magnesium gluconate sample. The Trivedi Effect[®] Treatment was provided by the group of eighteen renowned The Trivedi Effect[®] Energy Healers who participated in this study and performed the Trivedi Effect[®] Energy Treatment remotely. Eleven Energy Healers were remotely located in the U.S.A., four remotely located in Canada, two remotely located in Finland, and one of which was remotely located in Albania, while the test compound was located in the research laboratory of GVK Biosciences Pvt. Ltd., Hyderabad, India. This Trivedi Effect[®] Treatment was provided for 5 minutes through the Healer's Unique Energy Transmission process remotely to the test compound, which was kept under laboratory conditions. None of the Energy Healers in this study visited the laboratory in person, nor had any contact with the compounds. Similarly, the control compound was subjected to a "sham" healer for 5 minutes, under the same laboratory conditions. The sham healer did not have any knowledge about The Trivedi Effect[®] - Energy of Consciousness Healing Treatment. After that, the Trivedi Effect[®] Energy Treated and untreated samples were kept in similar sealed conditions and characterized thoroughly by LC-MS and NMR spectroscopy.

2.3. Liquid Chromatography Mass Spectrometry (LC-MS) Analysis

Liquid chromatography was performed using The Waters[®] ACQUITY UPLC, Milford, MA, USA equipped with a binary pump (The Waters[®] BSM HPLC pump), autosampler, column heater and a photo-diode array (PDA) detector. The column used for the study was a reversed phase Acquity BEH shield RP C18 (150 X 3.0 mm, 2.5 μ m). The column temperature was kept constant at 40°C. The mobile phase was 2mM ammonium acetate in water as mobile phase A and acetonitrile as mobile phase B. Chromatographic separation was achieved with following gradient program: 0 min – 5%B; 1 min – 5%B; 15 min - 97%B; 20 min – 97%B; 21 min – 5%B; 25 min – 5%B. The flow rate was at a constant flow rate of 0.4 mL/min. The control and Trivedi Effect[®] Energy Treated samples were dissolved in a mixture of water and methanol (60:40 v/v) to prepare a 1 mg/mL stock solution. An aliquot of 2 μ L of the stock solution was used for analysis by LC-ESI-MS and the total run time was 25 min. Mass spectrometric analysis was accompanied on a Triple Quad (Waters Quattro Premier XE, USA) mass spectrometer equipped with an electrospray ionization (ESI) source with the following parameters: electrospray capillary voltage 3.5 kV; source temperature 100°C; desolvation temperature 350°C; cone voltage 30 V; desolvation gas flow 1000 L/h and

cone gas flow 60 L/h. Nitrogen was used in the electrospray ionization source. The multiplier voltage was set at 650 V. LC-MS was taken in positive and negative ionization mode and with the full scan (m/z 50-1400). The total ion chromatogram, % peak area and mass spectrum of the individual peak (appeared in LC) were recorded.

2.4. Isotopic Abundance Ratio Analysis

The relative intensity of the peak in the mass spectra is directly proportional to the relative isotopic abundance of the molecule and the isotopic abundance ratio analysis was followed the scientific literature reported [41, 42] method described as below:

P_M stands for the relative peak intensity of the parent molecular ion [M^+] expressed in percentage. In other way, it indicates the probability to A elements having only one natural isotope in appreciable abundance (for e.g. ^{12}C , ^1H , ^{16}O , ^{24}Mg , etc.) contributions to the mass of the parent molecular ion [M^+].

P_{M+1} represents the relative peak intensity of the isotopic molecular ion [$(M+1)^+$] expressed in percentage

$$= (\text{no. of } ^{13}\text{C} \times 1.1\%) + (\text{no. of } ^{15}\text{N} \times 0.40\%) + (\text{no. of } ^2\text{H} \times 0.015\%) + (\text{no. of } ^{17}\text{O} \times 0.04\%) + (\text{no. of } ^{25}\text{Mg} \times 12.66\%)$$

i.e. the probability to $A + 1$ elements having an isotope that has one mass unit heavier than the most abundant isotope (for e.g. ^{13}C , ^2H , ^{17}O , ^{25}Mg , etc.) contributions to the mass of the isotopic molecular ion [$(M+1)^+$].

P_{M+2} represents the relative peak intensity of the isotopic molecular ion [$(M+2)^+$] expressed in the percentage

$$= (\text{no. of } ^{18}\text{O} \times 0.20\%) + (\text{no. of } ^{26}\text{Mg} \times 13.94\%)$$

i.e. the probability to have $A + 2$ elements having an isotope that has two mass unit heavier than the most abundant isotope (for e.g. ^{18}O , ^{26}Mg , etc.) contributions to the mass of isotopic molecular ion [$(M+2)^+$].

Table 1. The isotopic composition (*i.e.* the natural isotopic abundance) of the elements.

| Element | Symbol | Mass | % Natural Abundance | A+1 Factor | A+2 Factor |
|-----------|------------------|------|---------------------|-----------------------|-----------------------|
| Hydrogen | ^1H | 1 | 99.9885 | | |
| | ^2H | 2 | 0.0115 | 0.015n _H | |
| Carbon | ^{12}C | 12 | 98.892 | | |
| | ^{13}C | 13 | 1.108 | 1.1 n _C | |
| Oxygen | ^{16}O | 16 | 99.762 | | |
| | ^{17}O | 17 | 0.038 | 0.04 n _O | |
| | ^{18}O | 18 | 0.200 | | 0.20 n _O |
| Magnesium | ^{24}Mg | 24 | 78.99 | | |
| | ^{25}Mg | 25 | 10.00 | 12.66 n _{Mg} | |
| | ^{26}Mg | 26 | 11.01 | | 13.94 n _{Mg} |

A represents element, n represents the number of the element (*i.e.* C, H, O, Mg, etc.)

The value of the natural isotopic abundance of the elements used here for the theoretical calculation are achieved from the scientific literature and presented in the Table 1 [43, 44].

Isotopic abundance ratio for A + 1 elements = P_{M+1}/P_M

Similarly, isotopic abundance ratio for A + 2 elements = P_{M+2}/P_M

Percentage (%) change in isotopic abundance ratio = $[(IAR_{Treated} - IAR_{Control}) / IAR_{Control}] \times 100$ (1)

Where, $IAR_{Treated}$ = isotopic abundance ratio in the Biofield Energy Treated sample and $IAR_{Control}$ = isotopic abundance ratio in the control sample.

2.5. Nuclear Magnetic Resonance (NMR) Analysis

1H NMR spectra were recorded in a 400 MHz VARIAN FT-NMR spectrometer at room temperature. Data refer to solutions in D_2O with the residual solvent protons as internal

references. 1H NMR multiplicities were designated as singlet (s), doublet (d), triplet (t), multiplet (m), and broad (br). ^{13}C NMR spectra were measured at 100 MHz on a VARIAN FT-NMR spectrometer at room temperature. Chemical shifts (δ) were in parts per million (ppm) relative to the solvent's residual proton chemical shift (D_2O , $\delta = 4.65$ ppm) and solvent's residual carbon chemical shift (D_2O , $\delta = 0$ ppm).

3. Results and Discussion

3.1. Liquid Chromatography-Mass Spectrometry (LC-MS) Analysis

The liquid chromatograms of the control and Trivedi Effect® Biofield Energy Treated magnesium gluconate are presented in the Figure 1.

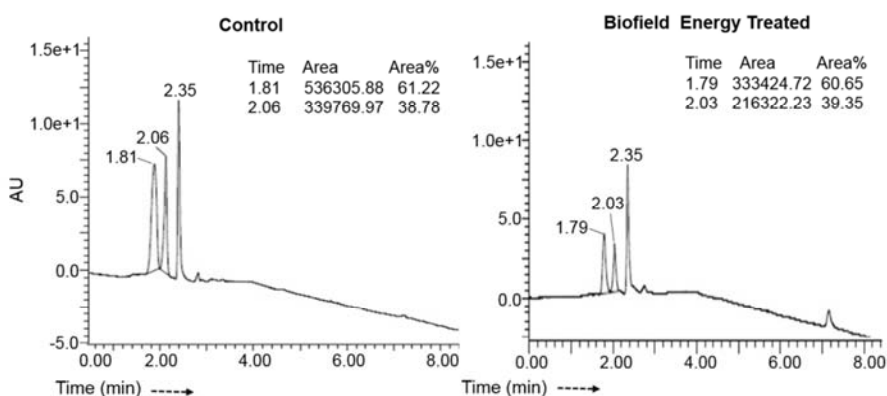


Figure 1. Liquid chromatograms of the control and Trivedi Effect® Biofield Energy Treated magnesium gluconate.

The ESI-MS spectra of the control and treated magnesium gluconate at corresponding the retention time (R_t) are shown in the Figures 2 and 3. The R_t of the mixture of water and methanol (60:40 v/v) was at 2.35 min. Beside this, the liquid chromatogram of the control sample showed two peaks indicating that at R_t of 1.81 and 2.06 min with the peak area% of 61.22% and 38.78%, respectively (Figure 1). On the other hand, the treated sample exhibited also two peaks at

R_t of 1.79 and 2.03 min with peak area% of 60.65% and 39.35%, respectively (Figure 1). These findings indicated that the polarity/affinity of the treated sample was unaltered as compared to the control sample. The ESI-MS spectra of the control and treated magnesium gluconate at R_t of 2.06 and 2.03 min (Figure 2) indicated the presence of the mass of magnesium gluconate adduct with methanol at m/z 447 $[M + CH_3OH + H]^+$ (calcd for $C_{13}H_{27}MgO_{15}^+$, 447).

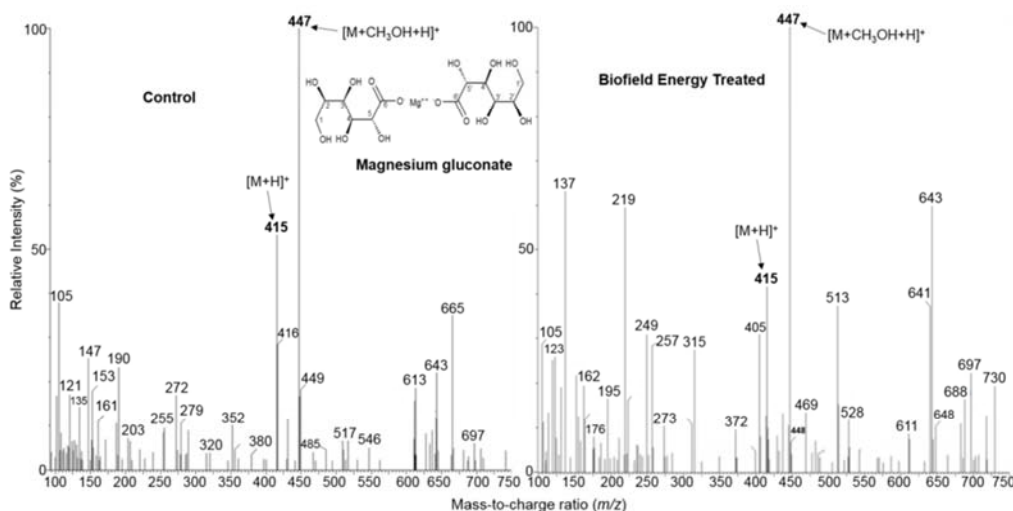


Figure 2. The ESI-MS spectra (Positive ionization mode) of the control and Biofield Energy Treated magnesium gluconate at the retention time 2.06 and 2.03 min, respectively.

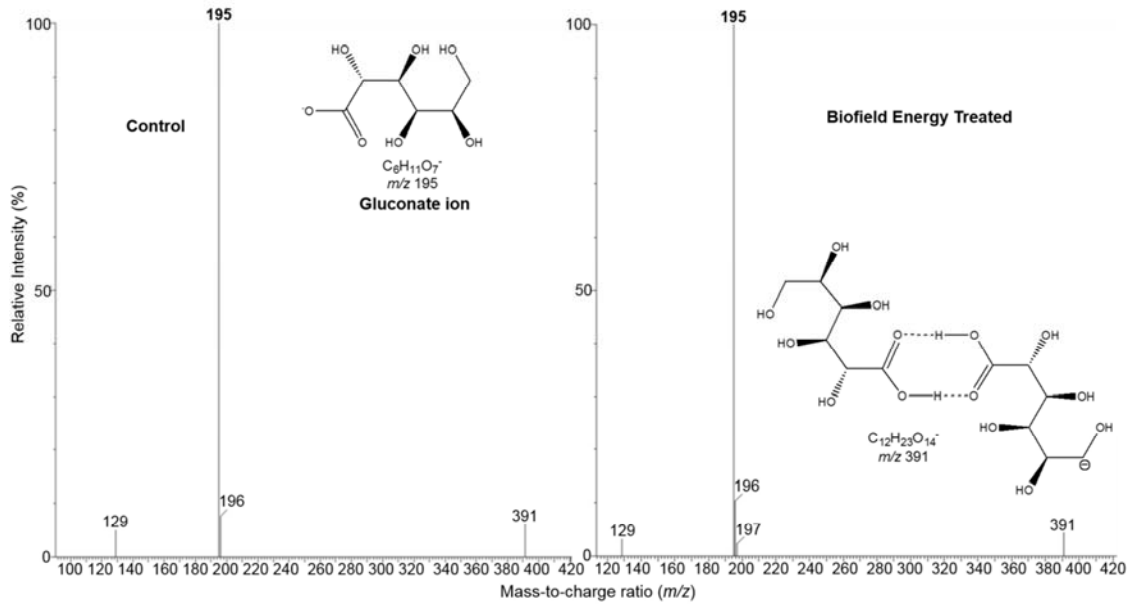


Figure 3. The ESI-MS spectra (Negative ionization) of the control and Biofield Energy Treated magnesium gluconate at the retention time 1.81 and 1.79 min, respectively.

There was also a peak for the protonated molecular ion at m/z 415 (calcd for $C_{12}H_{23}MgO_{14}^+$, 415) for magnesium gluconate (Figure 2).

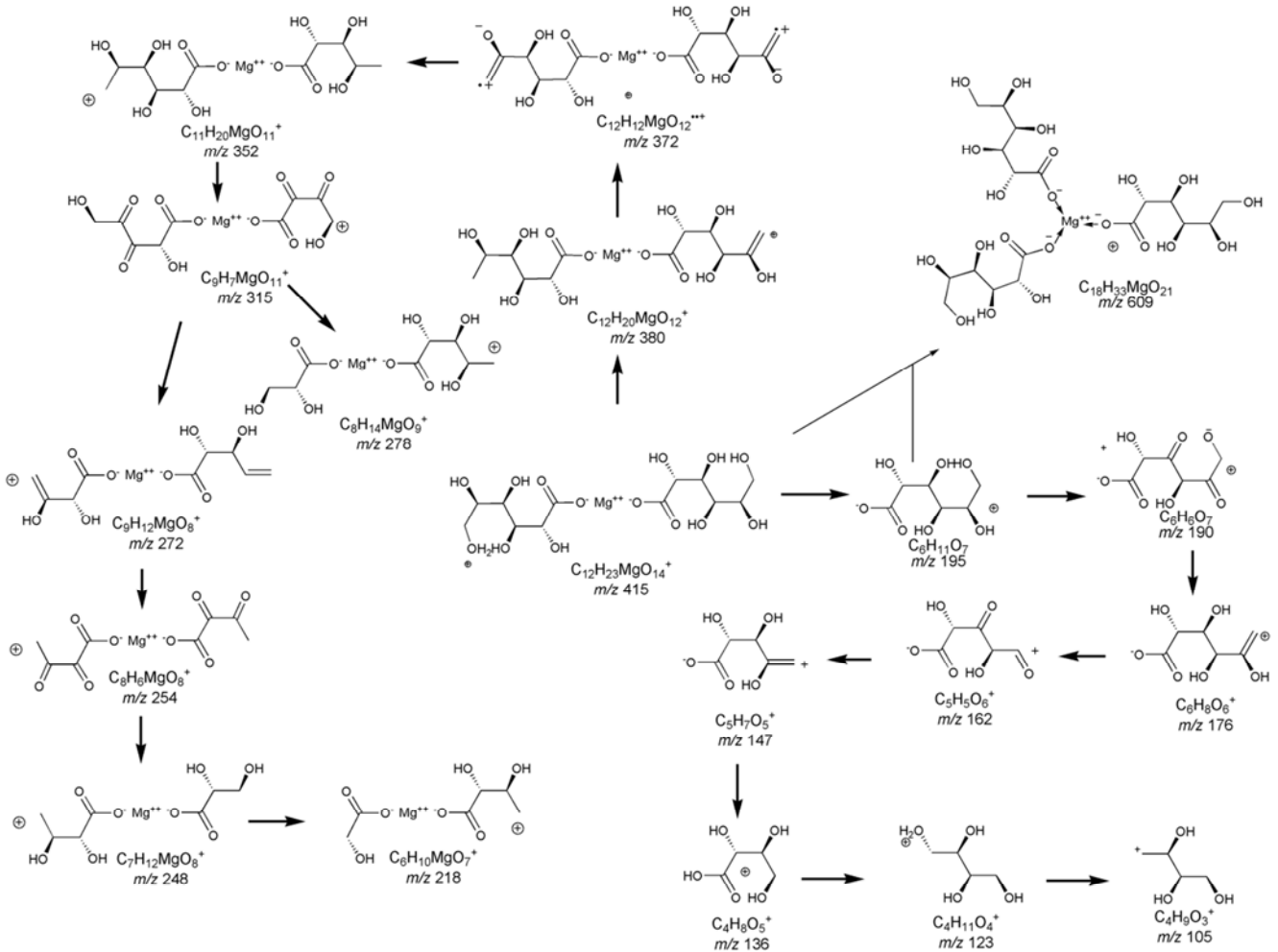


Figure 4. Proposed fragmentation pathway of magnesium gluconate.

The pseudo molecular ion magnesium gluconate at m/z 447 displayed 100% relative intensity. The characteristic fragmented ion peaks in the lower m/z region of the magnesium gluconate ion (m/z 415) were observed in the control sample at m/z 380, 352, 279, 272, 255, 190, 161, 147, 135, 121, and 105 due to the successive removal of water, CO and alkyl groups from $[M + H]^+$ and consequently, the internal molecular rearrangement, corresponded to the following ions $C_{12}H_{20}MgO_{12}^+$, $C_{11}H_{20}MgO_{11}^+$, $C_8H_{15}MgO_9^+$, $C_9H_{12}MgO_8^+$, $C_8H_7MgO_8^+$, $C_6H_6O_7^+$, $C_5H_4O_6^+$, $C_5H_7O_5^+$, $C_4H_7O_5^+$, $C_4H_9O_4^+$, and $C_4H_9O_3^+$ respectively as shown in Figure 4. The major ions observed in the higher m/z region of the control ESI-MS spectrum (Figure 2) were at m/z 613, 643 and 665. These mass indicated for the mass of the magnesium gluconate chelate with one gluconate ion through coordinate covalent bond ($C_{18}H_{33}MgO_{21}$, 609) as shown in Figure 4. But it existed in three different pseudo-molecular ions. First pseudo-molecular ion was at m/z 613 $[M + 4H]^+$ (calcd for $C_{18}H_{37}MgO_{21}^+$, 613). The second pseudo-molecular ion was due to the adduct formation with methanol at m/z 643 $[M + CH_3OH + H]^+$ (calcd for $C_{19}H_{38}MgO_{22}^+$, 643). The last pseudo-molecular ion was at m/z 665 (calcd for $C_{19}H_{37}Mg_2O_{22}^+$, 665) due to the adduct formation of $C_{18}H_{33}MgO_{21}$ with one Mg^{++} atom as well as with methanol. On the other hand, the ESI-MS spectrum of the treated sample at the retention time 2.03 min revealed the presence of the protonated magnesium gluconate ion at m/z 415 and 447 as similar to the control sample, but the fragmentation pattern and the relative peak intensities of the treated sample were different from the control sample. The distinctive fragmented ion peaks in the lower m/z region of the magnesium gluconate ion (m/z 415) were noticed in the treated sample at m/z 372, 315, 273, 257, 219, 195, 176, 162, 137, 123, and 105 corresponded to the molecular formula $C_{12}H_{12}MgO_{12}^{++}$, $C_9H_7MgO_{11}^+$, $C_9H_{13}MgO_8^+$, $C_8H_9MgO_8^+$, $C_6H_{11}MgO_7^+$, $C_6H_{11}O_7^+$, $C_6H_8O_6^+$, $C_5H_5O_6^+$, $C_4H_9O_5^+$, $C_4H_{11}O_4^+$, and $C_4H_9O_3^+$, respectively as shown in the Figure 4. The notable ions observed in the higher m/z region of the treated ESI-MS spectrum (Figure 2) were at m/z 611 and 643 corresponding to the molecular formula $C_{18}H_{35}MgO_{21}^+$ and $C_{19}H_{38}MgO_{22}^+$ that was due to the magnesium gluconate chelate with one gluconate ion. In addition, the ESI-MS of the control and treated magnesium gluconate at the retention time 1.81 and 1.79 min, respectively in the negative ionization mode (Figure 3) indicated only the presence of the gluconate ion at m/z 195 $[M]^-$ (calcd for $C_6H_{11}O_7^+$, 195) with 100% relative peak intensity. In the lower m/z region, a fragmented ion at m/z 129 corresponding molecular formula $C_6H_9O_3^-$ and the ion at m/z 391 which was due to the gluconate dimer ($C_{12}H_{23}O_{14}$) were also observed in their spectra. In this spectra, there was no alteration in fragmentation pattern of the gluconate ion observed in the control and Biofield Energy Treated samples except only the relative peak intensities.

3.2. Isotopic Abundance Ratio Analysis

The molecular formula of magnesium gluconate is $C_{12}H_{22}MgO_{14}$. The ESI-MS spectra of the control and

Biofield Energy Treated samples showed the mass of the protonated molecular ion at m/z 415 ($C_{12}H_{23}MgO_{14}^+$) showing 53.31% and 41.68% relative intensity, respectively along with adduct with methanol at m/z 447 ($C_{13}H_{27}MgO_{15}^+$) that displayed 100% relative intensity. The theoretical calculation of P_{M+1} and P_{M+2} for the protonated magnesium gluconate was presented as below:

$$P(^{13}C) = [(12 \times 1.1\%) \times 53.31\% \text{ (the actual size of the M}^+ \text{ peak)}] / 100\% = 7.04\%$$

$$P(^2H) = [(23 \times 0.015\%) \times 53.31\%] / 100\% = 0.18\%$$

$$P(^{17}O) = [(14 \times 0.04\%) \times 53.31\%] / 100\% = 0.30\%$$

$$P(^{25}Mg) = [(1 \times 12.66\%) \times 53.31\%] / 100\% = 6.75\%$$

P_{M+1} *i.e.* ^{13}C , 2H , ^{17}O , and ^{25}Mg contributions from ($C_{12}H_{23}MgO_{14}$) $^+$ to m/z 416 = 14.27%

From the above calculation, it has been found that ^{13}C and ^{25}Mg have major contribution to m/z 416.

In the similar approach, P_{M+2} can be calculated as follow:

$$P(^{18}O) = [(14 \times 0.20\%) \times 53.31\%] / 100\% = 1.49\%$$

$$P(^{26}Mg) = [(1 \times 13.94\%) \times 53.31\%] / 100\% = 7.43\%$$

So, P_{M+2} *i.e.* ^{18}O and ^{26}Mg contributions from ($C_{12}H_{23}MgO_{14}$) $^+$ to m/z 417 = 8.92%.

The experimental data of magnesium gluconate showed the different value from the calculated value due to the complexity in the structure. LC-MS spectra of the control and Biofield Energy Treated samples indicated the presence of the mass for the protonated magnesium gluconate itself (m/z 415) and adduct form with methanol (m/z 447) in positive ionization mode and the mass for the gluconate ion (m/z 195) in negative ionization mode. Hence, isotopic abundance ratio analysis for magnesium gluconate in the control and Biofield Energy Treated samples were calculated for its two forms *i.e.* adduct form at m/z 447 and protonated form at m/z 415 along with the gluconate ion at m/z 195. P_M , P_{M+1} , and P_{M+2} for magnesium gluconate ion and gluconate ion of the control and Biofield Energy Treated samples were obtained from the observed relative peak intensities of $[M]^+$, $[(M+1)]^+$, and $[(M+2)]^+$ peaks, respectively from their respective ESI-MS spectra and are presented in the Table 2 and 3. The percentage change of the isotopic abundance ratios (P_{M+1}/P_M and P_{M+2}/P_M) in the Biofield Energy Treated sample with respect to the control sample is shown in the Tables 2 and 3. The isotopic abundance ratio of P_{M+1}/P_M in two magnesium gluconate ion two forms at m/z 447 and 415 in the Biofield Energy Treated sample was significantly reduced by 59.82% and 55.44%, respectively with respect to the control sample (Table 2). Consequently, the percentage change in the isotopic abundance ratio of P_{M+2}/P_M was remarkably decreased in the magnesium gluconate pseudo-molecular ion at m/z 447 in the Biofield Energy Treated sample by 78.26% compared with the control sample (Table 2). So, ^{13}C , 2H , ^{17}O , and ^{25}Mg contributions from ($C_{13}H_{27}MgO_{15}$) $^+$ to m/z 448 as

well as from $(C_{12}H_{23}MgO_{14})^+$ to m/z 416; ^{18}O and ^{26}Mg contributions from $(C_{13}H_{27}MgO_{15})^+$ to m/z 449 in the Biofield

Energy Treated sample were significantly altered with respect to the control sample.

Table 2. Isotopic abundance analysis results of the two magnesium gluconate ion forms at m/z 447 and 415 in the control and Biofield Energy Treated sample.

| Parameter | Control sample | Biofield Energy Treated sample |
|---|----------------|--------------------------------|
| P_M at m/z 447 (%) | 100.00 | 100.00 |
| P_{M+1} at m/z 448 (%) | 16.60 | 6.67 |
| P_{M+1}/P_M | 0.1660 | 0.0667 |
| % Change of isotopic abundance ratio (P_{M+1}/P_M) with respect to the control sample | | -59.82 |
| P_{M+2} at m/z 449 (%) | 18.12 | 3.94 |
| P_{M+2}/P_M | 0.1812 | 0.0394 |
| % Change of isotopic abundance ratio (P_{M+2}/P_M) with respect to the control sample | | -78.26 |
| P_M at m/z 415 (%) | 53.31 | 41.68 |
| P_{M+1} at m/z 416 (%) | 28.25 | 9.84 |
| P_{M+1}/P_M | 0.5299 | 0.2361 |
| % Change of isotopic abundance ratio (P_{M+1}/P_M) with respect to the control sample | | -55.44 |

P_M = the relative peak intensity of the parent molecular ion $[M^+]$; P_{M+1} = the relative peak intensity of the isotopic molecular ion $[(M+1)^+]$, P_{M+2} = the relative peak intensity of the isotopic molecular ion $[(M+2)^+]$, and M = mass of the parent molecule.

The molecular formula of gluconate ion is $C_6H_{11}O_7$ and the molecular ion $[M]^+$ peak for the control sample showed 100% relative intensity. Hence, P_{M+1} can be calculated theoretically as described below:

$P(^{13}C) = [(6 \times 1.1\%) \times 100\% \text{ (the actual size of the } M^+ \text{ peak)}] / 100\% = 6.60\%$

$P(^2H) = [(11 \times 0.015\%) \times 100\%] / 100\% = 0.17\%$

$P(^{17}O) = [(7 \times 0.04\%) \times 100\%] / 100\% = 0.28\%$

P_{M+1} i.e. ^{13}C , 2H , and ^{17}O contributions from $(C_6H_{11}O_7)^+$ to m/z 196 = 7.05%

The obtained experimental value (Table 3) for the control sample was almost closed to the above calculated theoretical value.

Table 3. Isotopic abundance analysis result of the gluconate ion at m/z 195 in the control and Biofield Energy Treated samples.

| Parameter | Control sample | Biofield Energy Treated sample |
|---|----------------|--------------------------------|
| P_M at m/z 195 (%) | 100.00 | 100.00 |
| P_{M+1} at m/z 196 (%) | 7.55 | 10.37 |
| P_{M+1}/P_M | 0.0755 | 0.1037 |
| % Change of isotopic abundance ratio (P_{M+1}/P_M) with respect to the control sample | | 37.35 |

P_M = the relative peak intensity of the parent molecular ion $[M^+]$; P_{M+1} = the relative peak intensity of the isotopic molecular ion $[(M+1)^+]$, and M = mass of the parent molecule.

The isotopic abundance ratio of P_{M+1}/P_M in gluconate ion in the Biofield Energy Treated sample was significantly increased by 37.35% with respect to the control sample (Table 3). Hence, ^{13}C , 2H , and ^{17}O contributions from $(C_6H_{11}O_7)^+$ to m/z 196 was enhanced in the Biofield Energy Treated sample compared with the control sample.

Scientific literature [40-42, 45] reported that the vibrational energy is closely related with the reduced mass (μ) of the compound and the alteration of the vibrational energy can affect the several properties like physicochemical, thermal properties of the molecule. The relation between the vibrational energy and the reduced mass (μ) for a diatomic molecule is expressed as below [40, 45]:

$$E_o = \frac{h}{4\pi} \sqrt{\frac{f}{\mu}} \quad (2)$$

Where E_o = the vibrational energy of a harmonic oscillator at absolute zero or zero point energy

f = force constant

$$\mu = \text{reduced mass} = \frac{m_a m_b}{m_a + m_b} \quad (3)$$

Where m_a and m_b are the masses of the constituent atoms.

Table 4. Possible isotopic bond and their effect in the vibrational energy in magnesium gluconate molecule.

| Entry No. | Probable isotopic bond | Isotope type | Reduced mass (μ) | Zero point vibrational energy (E_o) |
|-----------|------------------------|--------------|------------------------|---|
| 1 | $^{12}C-^{12}C$ | Lighter | 6.00 | Higher |
| 2 | $^{13}C-^{12}C$ | Heavier | 6.26 | Smaller |
| 3 | $^1H-^{12}C$ | Lighter | 0.92 | Higher |
| 4 | $^2H-^{12}C$ | Heavier | 1.04 | Smaller |
| 5 | $^{12}C-^{16}O$ | Lighter | 6.86 | Higher |
| 6 | $^{13}C-^{16}O$ | Heavier | 7.17 | Smaller |
| 7 | $^{12}C-^{17}O$ | Heavier | 7.03 | Smaller |
| 8 | $^{12}C-^{18}O$ | Heavier | 7.20 | Smaller |
| 9 | $^{16}O-^1H$ | Lighter | 0.94 | Higher |
| 10 | $^{16}O-^2H$ | Heavier | 1.78 | Smaller |
| 11 | $^{24}Mg-^{16}O$ | Lighter | 9.60 | Higher |
| 12 | $^{25}Mg-^{16}O$ | Heavier | 9.76 | Smaller |
| 13 | $^{26}Mg-^{16}O$ | Heavier | 9.91 | Smaller |
| 14 | $^{24}Mg-^{17}O$ | Heavier | 9.95 | Smaller |
| 15 | $^{24}Mg-^{18}O$ | Heavier | 10.29 | Smaller |

The alteration in the isotopic abundance ratios of $^{13}C/^{12}C$

for C-O; $^2\text{H}/^1\text{H}$ for C-H and O-H bonds; $^{17}\text{O}/^{16}\text{O}$ and $^{18}\text{O}/^{16}\text{O}$ for C-O bond; $^{25}\text{Mg}/^{24}\text{Mg}$, $^{26}\text{Mg}/^{24}\text{Mg}$, $^{17}\text{O}/^{16}\text{O}$ and $^{18}\text{O}/^{16}\text{O}$ for Mg-O bond have the significant impact on the ground state vibrational energy of the molecule due to the higher reduced mass (μ) as shown in the Table 4 that leads to the isotope effects of the molecule.

Mass spectroscopic analysis of the several organic compounds revealed that the isotopic abundance of $[\text{M}+1]^+$ and $[\text{M}+2]^+$ ions were increased or decreased, thereby suggesting the change in number of neutrons in the molecule. It was then postulated to the alterations in atomic mass and atomic charge through possible mediation of neutrino oscillation [46, 47]. It is then assumed that The Trivedi Effect®- Consciousness Energy Healing Treatment might provide the required energy for the neutrino oscillations. The changes of neutrinos inside the molecule in turn modified the particle size, chemical reactivity, density, thermal behavior, selectivity, binding energy etc. [46].

Kinetic isotope effect that is resultant from the variation in

the isotopic abundance ratio of one of the atoms in the reactants in a chemical reaction is very useful to study the reaction mechanism as well as for understanding the enzymatic transition state and all aspects of enzyme mechanism that is supportive for designing enormously effective and specific inhibitors [40, 45, 48]. As magnesium is an essential cofactor for various enzymatic reactions, Biofield Energy Treated magnesium gluconate that had altered isotopic abundance ratio might be useful for the study of enzyme mechanism as well as assist in the designing of novel potent enzyme inhibitors.

3.3. Nuclear Magnetic Resonance (NMR) Analysis

The ^1H and ^{13}C NMR spectra of the control and Biofield Energy Treated magnesium gluconate are presented in the Figures 5 and 6, respectively. NMR assignments of the control and Biofield Energy Treated magnesium gluconate are presented in the Table 5.

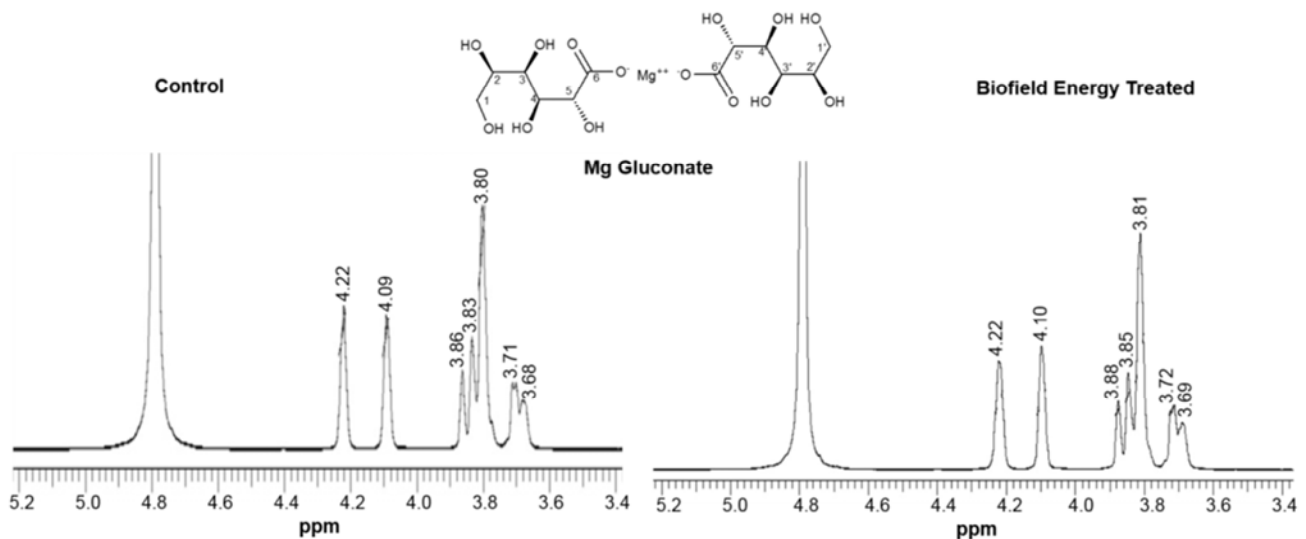


Figure 5. The ^1H NMR spectra of the control and Biofield Energy Treated magnesium gluconate.

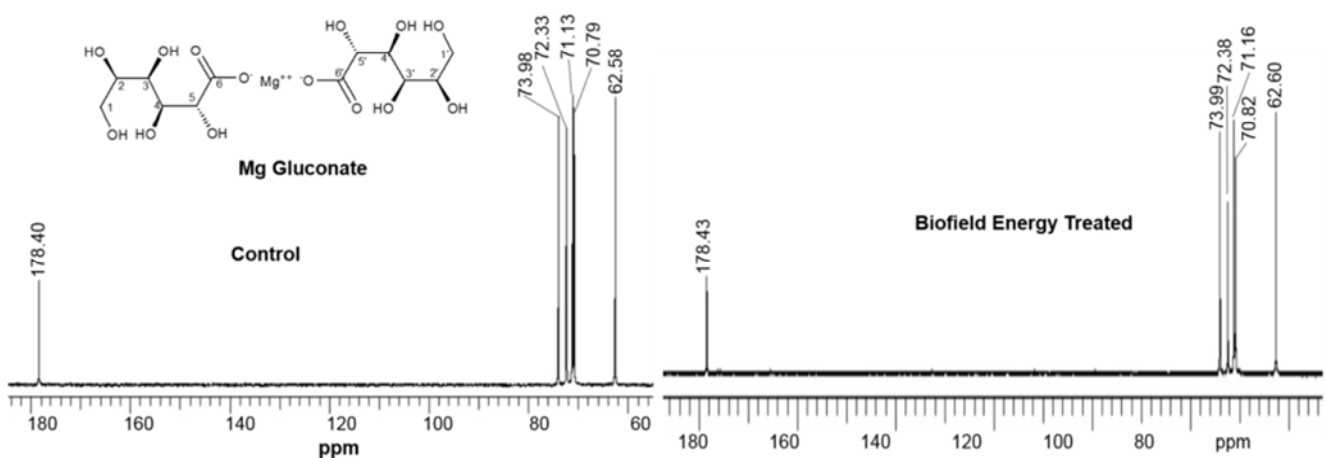


Figure 6. The ^{13}C NMR spectra of the control and Biofield Energy Treated magnesium gluconate.

Table 5. ^1H NMR and ^{13}C NMR spectroscopic data of both the control and Biofield Energy Treated of magnesium gluconate.

| Position | ^1H NMR δ (ppm) | | ^{13}C NMR δ (ppm) | | |
|----------|---------------------------------|----------------------------|------------------------------------|---------|------------------|
| | Number | Control | Biofield Treated | Control | Biofield Treated |
| 1, 1' | 4H* | 3.86 (br s), 3.68-3.71 (m) | 3.88 (br s), 3.69-3.71 (m) | 62.58 | 62.60 |
| 2, 2' | 2H* | 3.80 (br s) | 3.81 (br s) | 70.79 | 70.82 |
| 3, 3' | 2H* | 3.83 (br s) | 3.85 (br s) | 71.13 | 71.16 |
| 4, 4' | 2H | 4.09 (br s) | 4.10 (br s) | 72.33 | 72.38 |
| 5, 5' | 2H | 4.22 (br s) | 4.22 (br s) | 73.98 | 73.99 |
| 6, 6' | -- | -- | -- | 178.40 | 178.43 |

br- broad, s- singlet, and m- multiplet, * These assignments can be switched.

Although magnesium gluconate contains a large number of hydroxyl (OH) groups, the proton spectra of both the control and Biofield Energy Treated samples did not show any signal for the hydroxyl protons. The reason explained by the scientific literature [49] is that when deuterated water was used as solvent for spectra recording and the hydroxyl protons were replaced by deuterium from deuterated water. The signals for the protons coupling of CH_2 group and adjacent CH protons (2-5) in the gluconic acid portion were observed in the range of δ 3.60-4.20 ppm in the proton spectrum of sodium gluconate [49]. From the Table 5, it was found that the ^1H NMR spectra of both the control and Biofield Energy Treated samples exhibited the signals for CH_2 and CH groups in the range of δ 3.68-4.22 ppm. The carbon signals for CO group, CH_2 and CH groups in the ^{13}C NMR spectrum of the Biofield Energy Treated sample were unchanged compared with the control sample (Table 5). It was then concluded that the structure of the magnesium gluconate was remained unaltered due to the Biofield Energy Healing Treatment.

4. Conclusions

LC-ESI-MS analysis indicated that magnesium gluconate in the solution might be existed *in situ* of three forms, magnesium gluconate, gluconic acid and a chelate form of magnesium gluconate with gluconic acid by coordinate covalent bond. The ESI-MS spectra exposed the presence of the mass for the magnesium gluconate ion in two forms at m/z 447 (adduct form with methanol) and 415 in positive ionization mode and the mass for the gluconate ion at m/z 195 in negative ionization mode. The fragmentation pattern of the Trivedi Effect[®] Treated magnesium gluconate was found to be different from the control sample. Consequently, the LC-ESI-MS based isotopic abundance ratio analysis revealed that The Trivedi Effect[®] has the tremendous impact on the isotopic abundance ratios of P_{M+1}/P_M and P_{M+2}/P_M in the magnesium gluconate ion. The isotopic abundance ratio of P_{M+1}/P_M ($^2\text{H}/^1\text{H}$ or $^{13}\text{C}/^{12}\text{C}$ or $^{17}\text{O}/^{16}\text{O}$ or $^{25}\text{Mg}/^{24}\text{Mg}$) in two forms of magnesium gluconate ion at m/z 447 and 415 in the treated sample was significantly decreased by 59.82% and 55.44%, respectively with respect to the control sample. Subsequently, the percentage change of the isotopic abundance ratio of P_{M+2}/P_M ($^{18}\text{O}/^{16}\text{O}$ or $^{26}\text{Mg}/^{24}\text{Mg}$) was remarkably diminished in the magnesium gluconate ion at m/z 447 in the treated sample by 78.26% as compared to the control

sample. The isotopic abundance ratio of P_{M+1}/P_M ($^2\text{H}/^1\text{H}$ or $^{13}\text{C}/^{12}\text{C}$ or $^{17}\text{O}/^{16}\text{O}$) in gluconate ion in the treated sample was significantly increased by 37.35% with respect to the control sample. Briefly, ^{13}C , ^2H , ^{17}O , and ^{25}Mg contributions from $(\text{C}_{13}\text{H}_{27}\text{MgO}_{15})^+$ to m/z 448 as well as from $(\text{C}_{12}\text{H}_{23}\text{MgO}_{14})^+$ to m/z 416; ^{18}O and ^{26}Mg contributions from $(\text{C}_{13}\text{H}_{27}\text{MgO}_{15})^+$ to m/z 449 in the treated sample were significantly altered with respect to the control sample. ^{13}C , ^2H , and ^{17}O contributions from $(\text{C}_6\text{H}_{11}\text{O}_7)^+$ to m/z 196 was enhanced in the treated sample in comparison with the control sample. The treated sample might exhibit isotope effects such as altered physicochemical and thermal properties, rate of the reaction, selectivity and binding energy due to its changed isotopic abundance ratios of P_{M+1}/P_M and P_{M+2}/P_M as compared to the control sample. The treated magnesium gluconate might be helpful to understand the enzymatic reactions as well as design the novel potent enzyme inhibitors by using its kinetic isotope effects. Besides, The Trivedi Effect[®] - Consciousness Energy Healing Treatment could be a useful approach in the design of better nutraceutical and/or pharmaceutical formulations that can offer significant therapeutic responses against various diseases such as diabetes mellitus, allergies and septic shock, stress-related disorders like sleep disorder, insomnia, anxiety, depression, Attention Deficit Disorder (ADD), Attention Deficit Hyperactive Disorder (ADHD), mental restlessness (mind chattering), brain fog, low libido, impotency, lack of motivation, mood swings, fear of the future, confusion, migraines, headaches, forgetfulness, overwhelm, loneliness, worthlessness, indecisiveness, frustration, irritability, chronic fatigue, obsessive/compulsive behavior and panic attacks, inflammatory diseases and immunological disorders like Lupus, Systemic Lupus Erythematosus, Hashimoto Thyroiditis, Type 1 Diabetes, Asthma, Chronic peptic ulcers, Tuberculosis, Hepatitis, Chronic active hepatitis, Celiac Disease (gluten-sensitive enteropathy), Addison Disease, Crohn's disease, Graves' Disease, Pernicious and Aplastic Anemia, Sjogren Syndrome, Irritable Bowel Syndrome (IBS), Multiple Sclerosis, Rheumatoid arthritis, Chronic periodontitis, Ulcerative colitis, Chronic sinusitis, Myasthenia Gravis, Atherosclerosis, Vasculitis, Dermatitis, Diverticulitis, Rheumatoid Arthritis, Reactive Arthritis, Alopecia Areata, Psoriasis, Scleroderma, Fibromyalgia, Chronic Fatigue Syndrome and Vitiligo, aging-related diseases like cardiovascular disease, arthritis, cancer, Alzheimer's disease, dementia, cataracts, osteoporosis,

diabetes, hypertension, glaucoma, hearing loss, Parkinson's Disease, Huntington's Disease, Prion Disease, Motor Neurone Disease, Spinocerebellar Ataxia, Spinal muscular atrophy, Amyotrophic lateral sclerosis, Friedreich's Ataxia, Lewy Body Disease, chronic infections, and much more.

Abbreviations

A: Element; LC-MS: Liquid chromatography-mass spectrometry; GC-MS: Gas chromatography-mass spectrometry; M: Mass of the parent molecule; m/z : Mass-to-charge ratio; n: Number of the element; NMR: Nuclear magnetic resonance spectroscopy; P_M : The relative peak intensity of the parent molecular ion [M^+]; P_{M+1} : The relative peak intensity of isotopic molecular ion [(M+1)⁺]; P_{M+2} : The relative peak intensity of isotopic molecular ion [(M+2)⁺]; R_t : Retention time.

Acknowledgements

The authors are grateful to GVK Biosciences Pvt. Ltd., Trivedi Science, Trivedi Global, Inc. and Trivedi Master Wellness for their assistance and support during this work.

References

- [1] Heaton FW (1990) Role of magnesium in enzyme systems in metal ions in biological systems, In: Sigel H, Sigel A (Eds.), Volume 26: Compendium on magnesium and its role in biology, nutrition and physiology, Marcel Dekker Inc., New York.
- [2] Garfinkel L, Garfinkel D (1985) Magnesium regulation of the glycolytic pathway and the enzymes involved. *Magnesium* 4: 60-72.
- [3] Ramachandran S, Fontanille P, Pandey A, Larroche C (2006) Gluconic acid: Properties, applications and microbial production. *Food Technol Biotechnol* 44: 185-195.
- [4] Gröber U, Schmidt J, Kisters K (2015) Magnesium in prevention and therapy. *Nutrients* 7: 8199-8226.
- [5] William JH, Danziger J (2016) Magnesium deficiency and proton-pump inhibitor use: A clinical review. *J Clin Pharmacol* 56: 660-668.
- [6] Guerrero MP, Volpe SL, Mao JJ (2009) Therapeutic uses of magnesium. *Am Fam Physician* 80: 157-162.
- [7] Fleming TE, Mansmann Jr HC (1999) Methods and compositions for the prevention and treatment of diabetes mellitus. United States Patent 5871769, 1-10.
- [8] Fleming TE, Mansmann Jr HC (1999) Methods and compositions for the prevention and treatment of immunological disorders, inflammatory diseases and infections. United States Patent 5939394, 1-11.
- [9] Turner RJ, Dasilva KW, O'Connor C, van den Heuvel C, Vink R (2004) Magnesium gluconate offers no more protection than magnesium sulphate following diffuse traumatic brain injury in rats. *J Am Coll Nutr* 23: 541S-544S.
- [10] Weglicki WB (2000) Intravenous magnesium gluconate for treatment of conditions caused by excessive oxidative stress due to free radical distribution. United States Patent 6100297, 1-6.
- [11] Martin RW, Martin JN Jr, Pryor JA, Gaddy DK, Wisner WL, Morrison JC (1988) Comparison of oral ritodrine and magnesium gluconate for ambulatory tocolysis. *Am J Obstet Gynecol* 158: 1440-1445.
- [12] Coudray C, Rambeau M, Feillet-Coudray C, Gueux E, Tressol JC, Mazur A, Rayssiguier Y (2005) Study of magnesium bioavailability from ten organic and inorganic Mg salts in Mg-depleted rats using a stable isotope approach. *Magnes Res* 18: 215-223.
- [13] Stenger VJ (1999) Bioenergetic fields. *Sci Rev Alternative Med* 3.
- [14] Rogers, M (1989) "Nursing: A Science of Unitary Human Beings." In J.P. Riehl-Sisca (ed.) *Conceptual Models for Nursing Practice*. 3rd Edn. Norwalk: Appleton & Lange.
- [15] Rosa L, Rosa E, Sarner L, Barrett S (1998) A close look at therapeutic touch. *JAMA- J Am Med Assoc* 279: 1005-1010.
- [16] Warber SL, Cornelio D, Straughn, J, Kile G (2004) Biofield energy healing from the inside. *J Altern Complement Med* 10: 1107-1113.
- [17] Koithan M (2009) Introducing complementary and alternative therapies. *J Nurse Pract* 5: 18-20.
- [18] Trivedi MK, Patil S, Shettigar H, Gangwar M, Jana S (2015) *In vitro* evaluation of biofield treatment on cancer biomarkers involved in endometrial and prostate cancer cell lines. *J Cancer Sci Ther* 7: 253-257.
- [19] Trivedi MK, Patil S, Shettigar H, Mondal SC, Jana S (2015) The potential impact of biofield treatment on human brain tumor cells: A time-lapse video microscopy. *J Integr Oncol* 4: 141.
- [20] Trivedi MK, Branton A, Trivedi D, Nayak G, Mondal SC, Jana S (2015) Antimicrobial sensitivity, biochemical characteristics and biotyping of *Staphylococcus saprophyticus*: An impact of biofield energy treatment. *J Women's Health Care* 4: 271.
- [21] Trivedi MK, Branton A, Trivedi D, Nayak G, Bairwa K, Jana S (2015) *In vitro* evaluation of antifungal sensitivity assay of biofield energy treated fungi. *Fungal Genom Biol* 5: 125.
- [22] Trivedi MK, Branton A, Trivedi D, Nayak G, Mondal SC, Jana S (2015) Evaluation of antibiogram, genotype and phylogenetic analysis of biofield treated *Nocardia otitidis*. *Biol Syst Open Access* 4: 143.
- [23] Trivedi MK, Branton A, Trivedi D, Nayak G, Charan S, Jana S (2015) Phenotyping and 16S rDNA analysis after biofield treatment on *Citrobacter braakii*: A urinary pathogen. *J Clin Med Genom* 3: 129.
- [24] Trivedi MK, Patil S, Shettigar H, Bairwa K, Jana S (2015) Evaluation of phenotyping and genotyping characteristic of *Shigella sonnei* after biofield treatment. *J Biotechnol Biomater* 5: 196.
- [25] Trivedi MK, Branton A, Trivedi D, Nayak G, Mondal SC, Jana S (2015) Antibiogram, biochemical reactions and genotyping characterization of biofield treated *Staphylococcus aureus*. *American Journal of BioScience* 3: 212-220.

- [26] Trivedi MK, Branton A, Trivedi D, Nayak G, Bairwa K, Jana S (2015) Spectroscopic characterization of disulfiram and nicotinic acid after biofield treatment. *J Anal Bioanal Tech* 6: 265.
- [27] Trivedi MK, Patil S, Shettigar H, Singh R, Jana S (2015) An impact of biofield treatment on spectroscopic characterization of pharmaceutical compounds. *Mod Chem Appl* 3: 159.
- [28] Trivedi MK, Nayak G, Patil S, Tallapragada RM, Jana S, Mishra RK (2015) Bio-field treatment: An effective strategy to improve the quality of beef extract and meat infusion powder. *J Nutr Food Sci* 5: 389.
- [29] Trivedi MK, Tallapragada RM, Branton A, Trivedi D, Nayak G, Latiyal O, Mishra RK, Jana S (2015) Physicochemical characterization of biofield energy treated calcium carbonate powder. *American Journal of Health Research* 3: 368-375.
- [30] Trivedi MK, Branton A, Trivedi D, Nayak G, Mondal SC, Jana S (2015) Evaluation of plant growth regulator, immunity and DNA fingerprinting of biofield energy treated mustard seeds (*Brassica juncea*). *Agriculture, Forestry and Fisheries* 4: 269-274.
- [31] Trivedi MK, Branton A, Trivedi D, Nayak G, Mondal SC, Jana S (2015) Evaluation of biochemical marker - glutathione and DNA fingerprinting of biofield energy treated *Oryza sativa*. *American Journal of BioScience* 3: 243-248.
- [32] Trivedi MK, Nayak G, Patil S, Tallapragada RM, Latiyal O, Jana S (2015) Impact of biofield treatment on atomic and structural characteristics of barium titanate powder. *Ind Eng Manage* 4: 166.
- [33] Trivedi MK, Branton A, Trivedi D, Nayak G, Singh R, Jana S (2015) Physical, thermal and spectroscopic characterization of biofield treated *p*-chloro-*m*-cresol. *J Chem Eng Process Technol* 6: 249.
- [34] Trivedi MK, Branton A, Trivedi D, Nayak G, Singh R, Jana S (2015) Physicochemical and spectral characterization of biofield energy treated 4-methylbenzoic acid. *American Journal of Chemical Engineering* 3: 99-106.
- [35] Trivedi MK, Nayak G, Patil S, Tallapragada RM, Mishra R (2015) Influence of biofield treatment on physicochemical properties of hydroxyethyl cellulose and hydroxypropyl cellulose. *J Mol Pharm Org Process Res* 3: 126.
- [36] Trivedi MK, Branton A, Trivedi D, Nayak G, Saikia G, Jana S (2016) Determination of isotopic abundance of ^2H , ^{13}C , ^{18}O , and ^{37}Cl in biofield energy treated dichlorophenol isomers. *Science Journal of Analytical Chemistry* 4: 1-6.
- [37] Trivedi MK, Branton A, Trivedi D, Nayak G, Saikia G, Jana S (2015) Influence of biofield energy treatment on isotopic abundance ratio in aniline derivatives. *Mod Chem Appl* 3: 168.
- [38] Schellekens RC, Stellaard F, Woerdenbag HJ, Frijlink HW, Kosterink JG (2011) Applications of stable isotopes in clinical pharmacology. *Br J Clin Pharmacol* 72: 879-897.
- [39] Muccio Z, Jackson GP (2009) Isotope ratio mass spectrometry. *Analyst* 134: 213-222.
- [40] Vanhaecke F, Kyser K (2012) Isotopic composition of the elements In *Isotopic Analysis: Fundamentals and applications using ICP-MS (1stedn)*, Edited by Vanhaecke F, Degryse P. Wiley-VCH GmbH & Co. KGaA, Weinheim.
- [41] Trivedi MK, Branton A, Trivedi D, Nayak G, Panda P, Jana S (2016) Determination of isotopic abundance of $^{13}\text{C}/^{12}\text{C}$ or $^2\text{H}/^1\text{H}$ and $^{18}\text{O}/^{16}\text{O}$ in biofield energy treated 1-chloro-3-nitrobenzene (3-CNB) using gas chromatography-mass spectrometry. *Science Journal of Analytical Chemistry* 4: 42-51.
- [42] Trivedi MK, Branton A, Trivedi D, Nayak G, Sethi KK, Jana S (2016) Evaluation of isotopic abundance ratio in biofield energy treated nitrophenol derivatives using gas chromatography-mass spectrometry. *American Journal of Chemical Engineering* 4: 68-77.
- [43] Smith RM (2004) *Understanding Mass Spectra: A Basic Approach*, Second Edition, John Wiley & Sons, Inc, ISBN 0-471-42949-X.
- [44] Meija J, Coplen TB, Berglund M, Brand WA, De Bièvre P, Groning M, Holden NE, Irrgeher J, Loss RD, Walczyk T, Prohaska T (2016) Isotopic compositions of the elements 2013 (IUPAC technical Report). *Pure Appl Chem* 88: 293-306.
- [45] Asperger S (2003) *Chemical Kinetics and Inorganic Reaction Mechanisms* Springer science + Business media, New York.
- [46] Trivedi MK, Mohan TRR (2016) Biofield energy signals, energy transmission and neutrinos. *American Journal of Modern Physics* 5: 172-176.
- [47] Trivedi MK, Branton A, Trivedi D, Nayak G, Panda P, Jana S (2016) Mass spectrometric analysis of isotopic abundance ratio in biofield energy treated thymol. *Frontiers in Applied Chemistry* 1: 1-8.
- [48] Cleland WW (2003) The use of isotope effects to determine enzyme mechanisms. *J Biol Chem* 278: 51975-51984.
- [49] Nikolic VD, Illic DP, Nikolic LB, Stanojevic LP, Cakic MD, Tacic AD, Ilic-Stojanovic SS (2014) The synthesis and characterization of iron (II) gluconate. *Advanced technologies* 3: 16-24.